Epicardial multisite conduction blocks detected by equispaced electrode array and omnipolar technology in Brugada syndrome

Saverio Iacopino, MD,*[1] Federico Cecchini, MD,*[1] Alberto Tripodi, MD,[†]
Paolo Sorrenti, APRN,* Gennaro Fabiano, BSc,* Andrea Petretta, MD*

*From the *Electrophysiology Unit, Maria Cecilia Hospital GVM Care and Research, Cotignola, Italy, and [†]Department of Cardiovascular Surgery, Maria Cecilia Hospital GVM Care and Research, Cotignola, Italy.*

Introduction

Brugada syndrome (BrS) is an inherited channelopathy linked to an increased risk of developing malignant ventricular arrhythmias and sudden cardiac death in otherwise healthy individuals.[1] Currently, implantable cardioverter-defibrillator (ICD) is still the mainstay of treatment for BrS,[1] but for patients experiencing recurrent ICD shocks despite optimal medical therapy, radiofrequency (RF) transcatheter ablation of the arrhythmogenic substrate is an available option with promising results.[2–5] Although there is a generalized consensus in considering the right ventricular outflow tract (RVOT) epicardium as the locus harboring the pathologic substrate, the exact pathogenesis of BrS is still a matter of debate. The earliest theories related the tendency of developing ventricular arrhythmias to an abnormal and inhomogeneous repolarization giving rise to concealed phase 2 reentry in the epicardium[6,7]; however, recently there is more and more evidence that depolarization abnormalities such as slow conduction, conduction blocks, and excitation failure, caused by subtle RVOT epicardium fibrosis and gap-junction abnormalities, may play a paramount role in the arrhythmogenesis.[3,8,9]

The aforementioned alterations can be unmasked or magnified by sodium channel blockers (eg, ajmaline, flecainide, procainamide) and electrophysiologically are responsible for well-described electrogram (EGM) abnormalities such as low-amplitude epicardial EGMs (<1 mV) and/or late potentials (>120 ms) with multiple components (≥3) during sinus rhythm (SR).[3,4]

Nowadays identification of complex cardiac arrhythmia sources requires accurate substrate mapping, precise identification of time signal activation, and assessment of propagating wavefront. However, traditional bipolar signal recording has several limitations, and the novel omnipolar mapping technology (OT) was proved a helpful tool in complex mapping.[10]

KEY TEACHING POINTS

- Omnipolar mapping technology (OT) provides voltage, timing, and activation direction assessments independent of catheter orientation; it directly enables visualization of wavefronts on a mapping catheter as opposed to mapping a chamber from a collection of local activation times.
- Slow conduction areas and wave breaks within the Brugada syndrome (BrS) pathologic substrate under ajmaline administration can be precisely detected and visualized by means of OT mapping.
- The precise identification of the boundaries between pathologic and nonpathologic tissue substrate provided by the novel high-density omnipolar mapping may improve ablation efficacy.
- The detailed identification of the proper BrS substrate boundaries and the development of conduction slowing and conduction block under ajmaline administration may help clarify either the chaotic signal propagation or the mechanism of arrhythmia genesis.

Case report

A 72-year-old man with BrS and a previously implanted ICD was admitted to our clinic because of recurrent and appropriate ICD shocks despite optimal medical therapy.

KEYWORDS Brugada syndrome; Epicardial ablation; Minithoracotomy; Epicardial multisite conduction blocks; Depolarization failure; Omnipolar mapping technology; Activation map; Zero-fluoroscopy
(Heart Rhythm Case Reports 2023;9:12–16)

Funding Sources: This research did not receive any specific grant from funding agencies in the public, commercial, or not-for-profit sectors. Disclosures: Dr Iacopino, Dr Cecchini, Dr. Tripodi, G. Fabiano, P. Sorrenti, and A. Petretta do not have any conflict of interest to disclose. [1]Drs Iacopino and Cecchini provided equal first-level contribution in the realization of the manuscript. **Address reprint requests and correspondence:** Dr Saverio Iacopino, Electrophysiology Unit, Maria Cecilia Hospital, GVM Care and Research, Via Corriera 1, 48033 Cotignola (RA), Italy. E-mail address: iacopino@iol.it.

https://doi.org/10.1016/j.hrcr.2022.09.015

The patient was diagnosed with BrS at the age of 62. After his 20-year-old son's sudden death during sleep and evidence at the surface 12-lead electrocardiogram (ECG) of type III Brugada pattern (Figure 1, panel 2A), he underwent ajmaline test that unveiled a type I BrS ECG pattern (Figure 1, panel 2B). In 2012 he underwent ICD implantation because of his family history of sudden cardiac death and 3 past episodes of uninvestigated syncope during rest.

After about 9 uneventful years, the patient had a first appropriate ICD shock for ventricular fibrillation (VF) (Figure 1, panel 1). Invasive coronary angiography, intracoronary acetylcholine provocation testing, and transthoracic echocardiography turned out to be normal; moreover, hematochemical blood tests ruled out electrolyte abnormalities and inflammatory states. Unfortunately, despite antiarrhythmic therapy with quinidine (500 mg 3 times daily), a few weeks later the patient experienced another episode of VF promptly recognized and treated with DC shocks by the ICD. He was then readmitted to our hospital for epicardial ablation of the arrhythmogenic substrate with the use of an equispaced electrode array with omnipolar mapping technology.

After informed consent had been gained, the procedure was performed in the hybrid surgical room under general anesthesia and invasive arterial pressure monitoring. We previously described our zero-fluoroscopy hybrid minithoracotomy approach for BrS epicardial ablation.[11]

Briefly, pericardial access was achieved via left anterior minithoracotomy and a skin incision was conducted along the upper edge of the areola, overlying the third left intercostal space. After dissection of the external and internal intercostal muscles, discontinuation of lung ventilation was applied to displace the lung with a tissue retractor, allowing the pericardial space to be visualized and entered over the right ventricle (RV). Simultaneously, 2 right femoral venous accesses were obtained under echo-guidance by a second independent operator. An Advisor HD Grid multipolar mapping catheter (Abbott, Chicago, IL) was used to create a high-density bipolar and omnipolar map of the RV and RVOT endocardium during SR and a quadripolar diagnostic catheter was advanced up to the RV apex.

Following the endocardial map, which demonstrated the presence of healthy tissue, the multipolar mapping catheter was placed on the epicardium through the minithoracotomy access and directly manipulated by the physician by holding it with the fingers or a sawtell forceps. The 3-dimensional (3D) epicardial RVOT surface was then reconstructed with the EnSite X (Abbott, Chicago, IL), exploiting its magnetic navigation properties. Bipolar, HD wave, and OT maps were performed in SR, under baseline condition (pre–ajmaline infusion) and during ajmaline infusion/washout (1 mg/kg in 5 minutes).

At baseline, no areas of abnormal EGMs could be detected on the anterior aspect of the epicardial RVOT. During ajmaline infusion a Brugada type I pattern was unmasked and an area of low-amplitude fractionated and late EGMs expanded along the epicardial RVOT and RV anterior wall to cover a

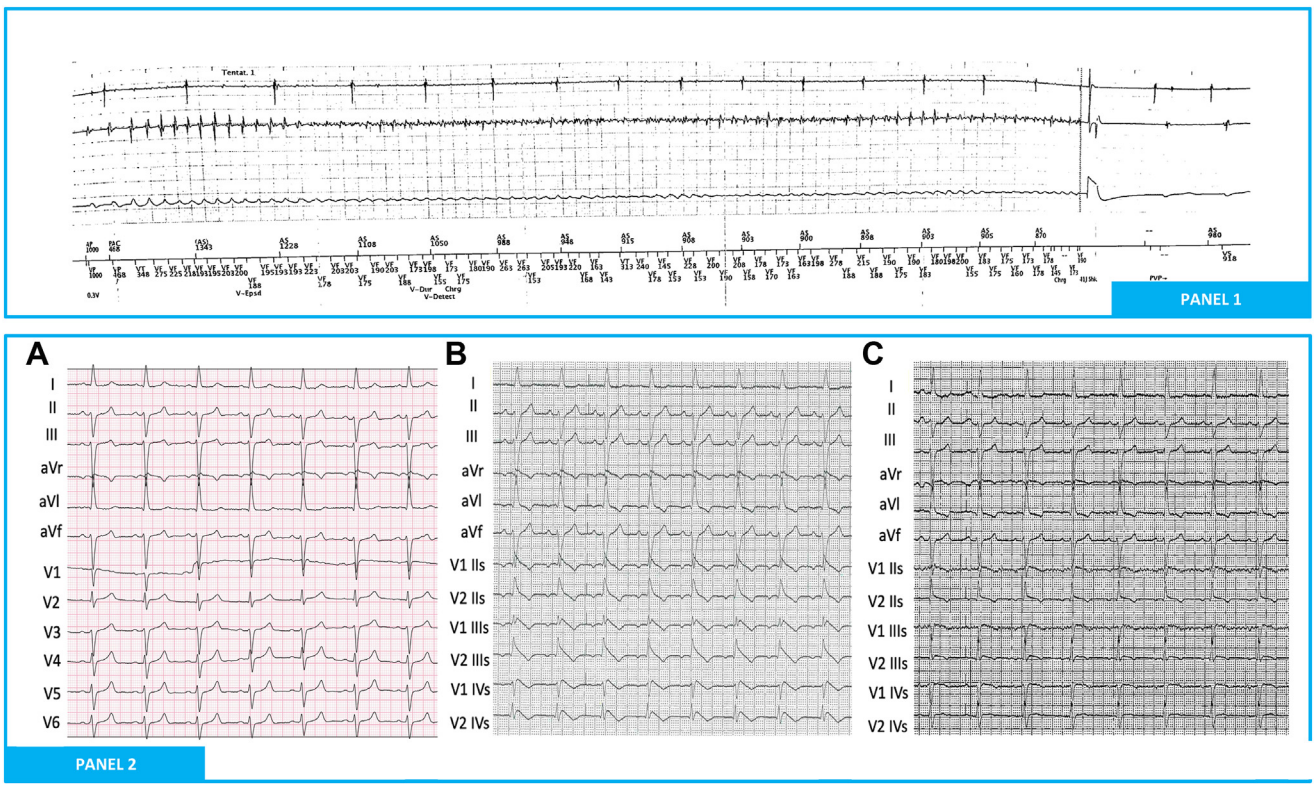

Figure 1 **Panel 1:** Ventricular fibrillation initiation interrupted by an appropriate implantable cardioverter-defibrillator shock. **Panel 2: A:** Basal electrocardiogram (ECG); **B:** unmasking of type 1 Brugada syndrome (BrS) ECG pattern during ajmaline infusion; **C:** disappearance of type 1 BrS ECG pattern during a further ajmaline administration 3 months after epicardial ablation of the arrhythmogenic substrate.

surface of 17 cm^2. The analysis of omnipolar maps revealed the appearance of several multisite conduction blocks in this epicardial pathologic area: conduction blocks were discovered either in the central part of or in proximity of the border zone between the normal and low-voltage areas (normal and long-fragmented potential) (Figure 2 and panel 1 of Figure 3). The baseline maps were inspected to compare conduction direction and we noted that the line of conduction block that appeared after ajmaline infusion was not present before.

All the pathologic EGMs inside the area were tagged and targeted for RF ablation carried out with a contact force sensor (TactiCath, Abbott) in a temperature-controlled mode (max 43°C) with a power limit of 30 W until reaching a lesion index of 5.[11] The total number of RF applications was 35 for a total RF time of 1600 seconds.

After ablation, a second ajmaline administration did not induce type 1 BrS ECG pattern, and the contemporaneous epicardial remap showed abatement of all the abnormal EGMs previously detected, replaced by a large scar area (Figure 3, panel 2).

A final programmed ventricular stimulation protocol failed to induce any ventricular arrhythmia. The patient was discharged 5 days after the procedure, without complications.

After 5 months of follow-up, the patient did not experience any arrhythmia recurrence and a further ajmaline test was negative for type 1 BrS ECG pattern induction (Figure 1, panel 2C).

Discussion

OT provides electrode orientation–independent cardiac wavefront trajectory and speed at a single location for each cardiac cycle.[10] Both unipolar and bipolar signals read by each electrode triplets (omnipole) are used to obtain the true voltage signal, direction, and speed of front propagation. An omnipole resolves signals from all possible simultaneous bipoles (from every direction around the mapping location) from the electric field generated by the traveling wave and could provide a definitive assessment of the local cardiac wave properties.[12] The latter can be challenging to determine with traditional bipolar methods because ambiguity arises from the orientation and placement of the electrode in the area of interest. Traditional bipolar-based substrate maps are heavily influenced by the direction of a wavefront to the mapping bipole. Recently, Porta-Sánchez and colleagues[13] evaluated high-resolution, orientation-independent peak-to-peak voltage maps obtained with an equispaced electrode array and omnipolar EGMs in the endocardium of 10 pigs. Omnipolar EGMs better delineate infarcted and noninfarcted areas than traditional bipolar EGMs from both orientations.

To the best of our knowledge, we reported the first visualization of wavefront fragmentation and conduction blocks in the epicardial BrS arrhythmogenic substrate obtained with a 3D mapping system and omnipolar high-density mapping.

Our omnipolar substrate mapping revealed, under ajmaline administration, several areas of disorganized propagation and conduction block (Figure 2, panel 1, and Supplementary Video); interestingly, those areas were located either in the center of the pathologic RVOT or at the border between the pathologic and the nonpathologic RVOT areas outlined during ajmaline administration. OT allowed a fast, detailed, and real-time assessment of the arrhythmogenic substrate during BrS ablation procedure. Information on direction wavefront (Figure 2, *green arrows*) pointed out areas of conduction block and areas in which conduction direction drastically changed before and after ajmaline administration (Figure 2, panel 2). Traditional bipolar maps lack this information, which can be useful for a comprehensive

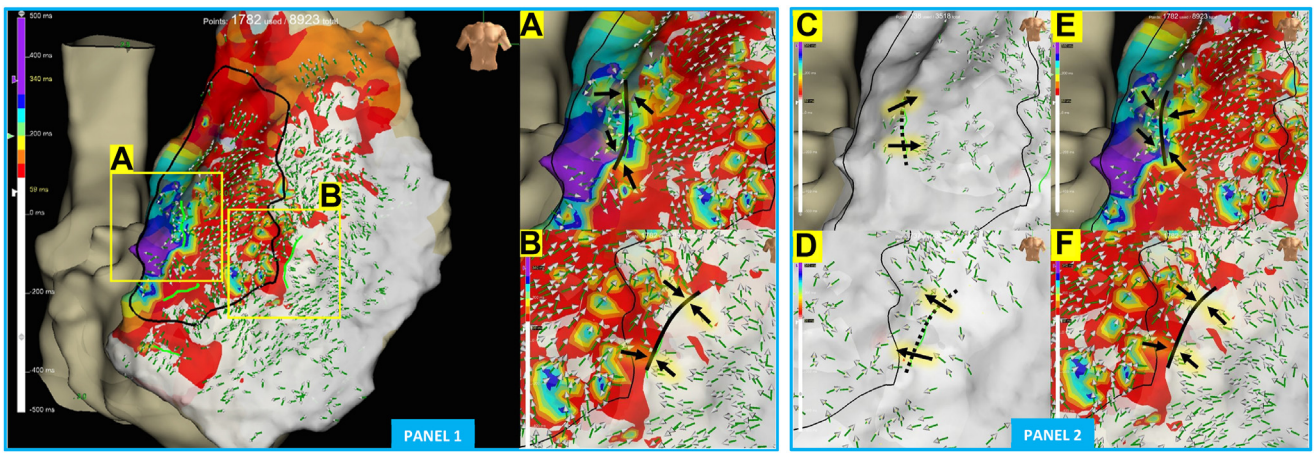

Figure 2 **Panel 1:** Omnipolar local activation map (LAT) performed after the infusion of ajmaline with signal propagation through the epicardial Brugada syndrome (BrS) substrate (*green arrows* represent the local direction of signal propagation). Subpanels **A** and **B** represent an enlargement of 2 right ventricular outflow tract areas where conduction block lines (*black lines and arrows*) appeared after administration of ajmaline. **Panel 2:** Effects of ajmaline infusion on signal propagation in the BrS substrate. Subpanels **C** and **D** depict omnipolar LAT maps performed under baseline conditions while subpanels **E** and **F** show the respective changes during ajmaline infusion (*black lines and arrows*). Differences can be seen in ajmaline in the direction of signal propagation and the appearance of conduction block lines (*black lines and arrows*) in the vicinity of the areas with later and fragmented signals (*blue-violet areas*) and at the border areas (*red-white areas*).

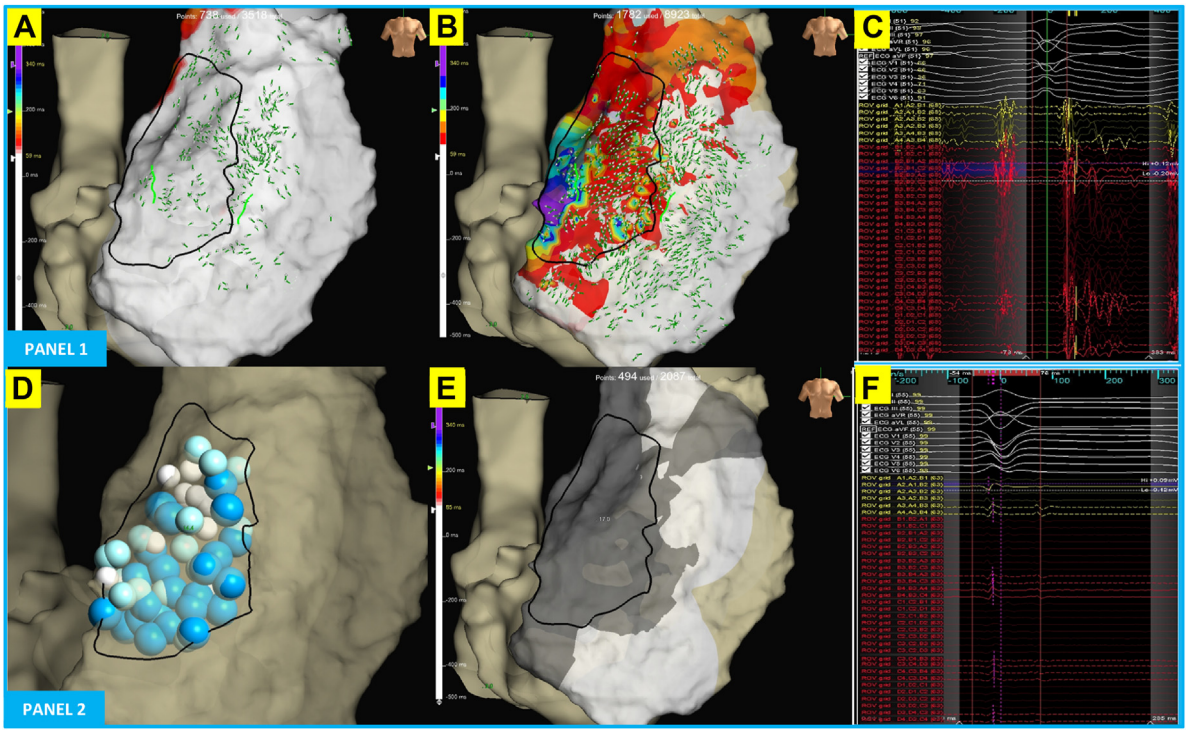

Figure 3 **Panel 1: A,B:** Omnipolar local activation map (LAT) performed during baseline condition in sinus rhythm (**A**) and during ajmaline administration (**B**); the black line represents the pathologic area tagged for ablation. **C:** Electrogram (EGM) equivalents of wave breaks (multiple deflections separated by isoelectric lines) and slow/anisotropic conduction (long fractionated potentials) over the yellow-outlined area. **Panel 2:** Radiofrequency ablation of the Brugada syndrome (BrS) arrhythmogenic substrate. **D:** Each sphere corresponds to a point-by-point lesion index-guided ablation. **E:** Remap postablation during ajmaline administration showed complete abolition of the BrS arrhythmogenic substrate. **F:** No abnormal EGM could be found during a further ajmaline administration.

characterization of the ablation target. Presence of chaotic depolarization may provide a functional substrate for phase 2 reentry and degeneration of ventricular tachycardia into VF. Moreover, precise refinement of the pathologic RVOT borders may be crucial, and failure to ablate even a small pathologic surface could be responsible for arrhythmic relapses during the follow-up.[3,4]

Our results are in line with the ones reported for RV-RVOT by Lambiase and colleagues[14] using an intracardiac noncontact mapping array and isochronal mapping. During a ventricular S1-S2 stimulation protocol the authors found a significant conduction delay in the RVOT of BrS subjects, which was not apparent in healthy controls; moreover, the same regions of delayed conduction gave rise to wavefront fragmentation and lines of blocks that led to polymorphic ventricular tachycardia that degenerated into VF in 5 out of 18 patients affected by BrS. This arrhythmogenic behavior has been recently reported also by Haïssaguerre and colleagues[8] and Nademanee and colleagues[15]: localized block occurs at multiple sites from a single premature stimulus or during sodium channel blocker infusion and could be responsible for VF initiation.

Conclusion

Omnipolar technology mapping may be a useful tool in BrS ablation to instantly determine and visualize the true signal voltage, its direction, and speed of activation with superior efficiency and less ambiguity than the standard bipolar method. The latter information may help clarify the chaotic signal propagation and wave breaks in BrS as well as better delineate the boundary between pathologic and nonpathologic areas during sodium channel blocker administration. Displaying a beat-to-beat 3D map of signal propagation OT may also help clarify the genesis of ventricular arrhythmias which, up to now, has never been visualized on an epicardial map.

Appendix

Supplementary Data

Supplementary data associated with this article can be found in the online version at https://doi.org/10.1016/j.hrcr.2022.09.015.

References

1. Priori SG, Blomström-Lundqvist C, Mazzanti A, et al. 2015 ESC Guidelines for the management of patients with ventricular arrhythmias and the prevention of sudden cardiac death: The Task Force for the Management of Patients with Ventricular Arrhythmias and the Prevention of Sudden Cardiac Death of the European Society of Cardiology (ESC) Endorsed by: Association for European Paediatric and Congenital Cardiology (AEPC). Eur Heart J 2015;36:2793–2867.
2. Nademanee K, Veerakul G, Chandanamattha P, et al. Prevention of ventricular fibrillation episodes in Brugada syndrome by catheter ablation over the anterior right ventricular outflow tract epicardium. Circulation 2011;123:1270–1279.
3. Zhang P, Tung R, Zhang Z, et al. Characterization of the epicardial substrate for catheter ablation of Brugada syndrome. Heart Rhythm 2016;13:2151–2158.
4. Pappone C, Brugada J, Vicedomini G, et al. Electrical substrate elimination in 135 consecutive patients with Brugada syndrome. Circ Arrhythm Electrophysiol 2017;10:e005053.

5. Salghetti F, de Asmundis C, Sieira J, et al. Hybrid thoracoscopic epicardial ablation of right ventricular outflow tract in patients with Brugada syndrome. Heart Rhythm 2019;16:879–887.
6. Antzelevitch C. Brugada syndrome. Pacing Clin Electrophysiol 2006;29:1130–1159.
7. Szél T, Antzelevitch C. Abnormal repolarization as the basis for late potentials and fractionated electrograms recorded from epicardium in experimental models of Brugada syndrome. J Am Coll Cardiol 2014;63:2037–2045.
8. Haïssaguerre M, Nademanee K, Sacher F, et al. Multisite conduction block in the epicardial substrate of Brugada syndrome. Heart Rhythm 2022;19:417–426.
9. Nademanee K, Raju H, de Noronha SV, et al. Fibrosis, connexin-43, and conduction abnormalities in the Brugada syndrome. J Am Coll Cardiol 2015; 66:1976–1986.
10. Massé S, Magtibay K, Jackson N, et al. Resolving myocardial activation with novel omnipolar electrograms. Circ Arrhythm Electrophysiol 2016;9:e004107.
11. Cecchini F, Iacopino S, Tripodi A, et al. Hybrid minithoracotomy approach for zero-fluoroscopy epicardial ablation of the arrhythmogenic substrate in Brugada syndrome. HeartRhythm Case Rep 2022;8:562–566.
12. Deno DC, Bhaskaran A, Morgan DJ, et al. High-resolution, live, directional mapping. Heart Rhythm 2020;17:1621–1628.
13. Porta-Sánchez A, Magtibay K, Nayyar S, et al. Omnipolarity applied to equispaced electrode array for ventricular tachycardia substrate mapping. Europace 2019;21:813–821.
14. Lambiase PD, Ahmed AK, Ciaccio EJ, et al. High-density substrate mapping in Brugada syndrome: combined role of conduction and repolarization heterogeneities in arrhythmogenesis. Circulation 2009;120:106–117.
15. Nademanee K, Veerakul G, Nogami A, et al. Mechanism of the effects of sodium channel blockade on the arrhythmogenic substrate of Brugada syndrome. Heart Rhythm 2022;19:407–416.